ChemComm

COMMUNICATION

View Article Online
View Journal | View Issue

Cite this: *Chem. Commun.*, 2014, **50**, 14851

Received 30th July 2014,
Accepted 6th October 2014

DOI: 10.1039/c4cc05929h

www.rsc.org/chemcomm

Direct exfoliation of carbon allotropes with structural analogues of self-assembled nanostructures and their photovoltaic applications†

Woochul Lee,‡[a] Dong-Woo Lee,‡[a] Myongsoo Lee*[b] and Jong-In Hong*[a]

Aromatic amphiphiles were self-assembled into 2-D nanosheets and 1-D nanofibers by systematically varying the volume fraction of the hydrophilic coils, which enabled the direct exfoliation of carbon allotropes with high quality and quantity. A 2-D nanosheet structure was introduced as the hole transporting layer for improving the performance of organic photovoltaic devices.

Carbon allotropes represent a group of attractive nanostructures with remarkable material properties and various optoelectronic applications such as organic field-effect transistors, and organic photovoltaic cells.[1] However, carbon allotropes in optoelectronic device applications face major limitations because of extremely low solubility in the solvent phase.[2] To attain processability in optoelectronic devices, a variety of exfoliation methods of carbon allotropes has been developed so far.[3] Recently, a laser based green technique was also developed for exfoliation of graphite into graphene and related 2D materials and for unzipping of carbon nanotubes to graphene nanoribbons.[4] In particular, the non-covalent functionalization of carbon allotropes, without causing damage to their intrinsic properties, is one of the most attractive exfoliation methods and has been reported by many research groups.[5] Among various non-covalent functionalization methods, the most widespread is that of small-molecule surfactant-supported functionalization. The solvophilic moieties in surfactants are oriented towards the solvent phase, while aromatic anchor groups, such as pyrene,[3a,6] porphyrin or phthalocyanine,[3a,7] are adsorbed on the surface of the carbon nanotube (CNT) or graphene (G) through π–π interactions. Many small-molecule surfactants are known to disperse CNT and G at low concentrations (<1 mg mL^{-1}).[8] Recently, the Lee group demonstrated that an aromatic amphiphile with an aromatic molecular sheet based on four pyrene units could selectively exfoliate graphite powder into 2-D G sheets in aqueous media while the 1-D single-wall carbon nanotube (SWNT) could not be dispersed in aqueous solution.[9] An amphiphilic perylene dye enabled the dispersion and debundling of SWNTs in aqueous media.[10] A series of porphyrin derivatives were used as an effective dispersant for SWNTs in DMF.[11] Moreover, the direct exfoliation of graphite to G in an aqueous solvent was realized through π–π interactions with the diazaperopyrenium dication.[12] These studies showed that single molecule-based surfactants are an attractive candidate for the exfoliation of structurally analogous carbon allotropes. These results stimulated us to rationally design a simple way for the exfoliation of carbon allotropes by structurally analogous nanostructures self-assembled from small-molecule amphiphiles comprising a rigid hydrophobic aromatic rod and flexible hydrophilic coil segments, because the self-assembly of amphiphilic molecules into 1-D nanofibers or 2-D nanosheets depends on the relative volume fraction of hydrophobic and hydrophilic units[13] without changing the chemical structure of the rigid aromatic core unit of rigid-flexible block molecules.[14]

In this communication, we report on amphiphilic molecules, their self-assembly, and the application of the self-assembled nanostructures to organic photovoltaic (OPV) devices (Fig. 1a). The amphiphilic molecules are based on a phenyl-thiophene aromatic rod, which is grafted by a hydrophilic polyether dendron at one end and a hydrophobic branch at the other end. The amphiphilic molecules self-assembled into 1-D nanofibers and 2-D nanosheets depending on the relative volume fraction of the hydrophilic polyether unit (R, Fig. 1a). Furthermore, the respective self-assembled nanostructures enabled a direct exfoliation of carbon allotropes at a high concentration (>1 mg mL^{-1}) (Fig. 1b). In particular, the blended mixture of a self-assembled nanosheet structure with graphite was successfully introduced into a poly(3,4-ethylenedioxythiophene):poly(styrene sulfonate) (PEDOT:PSS) hole transport layer (HTL) to improve the performance of OPVs.

A regioregular alternating aromatic segment of compounds **1–3**, containing both phenylene and thienylene subunits, is expected to allow for a unique conformational behavior in an aqueous solution.[15]

[a] *Department of Chemistry, Seoul National University, 1 Gwanak-ro, Gwanak-gu, Seoul 151-747, Korea. E-mail: jihong@snu.ac.kr*
[b] *State Key Lab of Supramolecular Structure and Materials, College of Chemistry, Jilin University, Changchun 130012, China. E-mail: mslee@jlu.edu.cn*

† Electronic supplementary information (ESI) available: Experimental details, AFM images, TEM images, device fabrication and characterization. See DOI: 10.1039/c4cc05929h

‡ These authors contributed equally to this work.

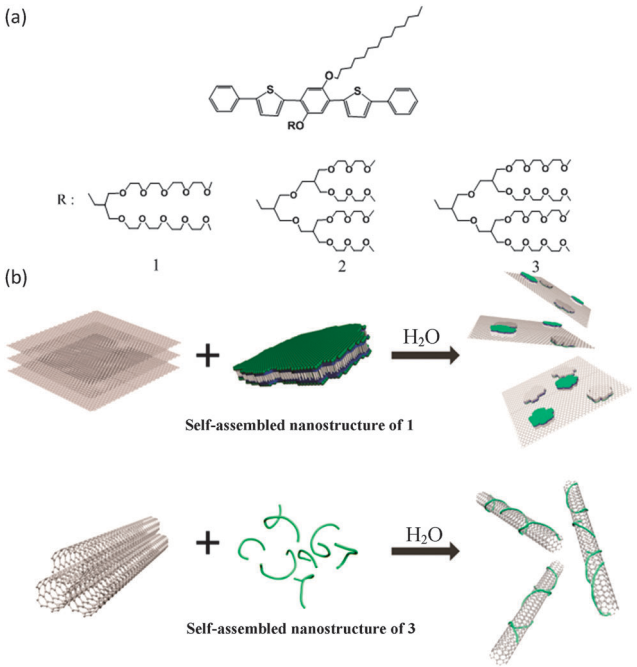

Fig. 1 (a) Chemical structures of amphiphiles **1**, **2**, and **3**. (b) Schematic representation of the dispersion of G/SWNT with the self-assembled nanostructures of **1** and **3**, respectively.

In addition, it is also expected that increasing the volume fraction of the hydrophilic chains would induce the unique nanostructure to relieve steric crowding at the interfaces between the aromatic rod and the hydrophilic coils.[16] Details of the synthesis of compounds **1**–**3** and their spectral data are provided in the ESI.† Aggregation behavior of these amphiphiles was studied in aqueous solution using transmission electron microscopy (TEM). In addition, cryogenic transmission electron microscopy (cryo-TEM) experiments were performed to confirm the formation of self-assembled nanostructures in bulk solution (Fig. S1, ESI†). The micrographs in Fig. 2 were obtained from 0.05 wt% (w/v) aqueous solutions of **1**, **2**, and **3** cast onto the TEM grid. The TEM image was negatively stained with uranyl acetate. As shown in the TEM image of solution **1** in Fig. 2a, 2-D nanosheets can be seen clearly, which was further confirmed by cryo-TEM images (Fig. 2b). Moreover, the section analysis of the atomic force microscopy (AFM) image of **1** shows that the thickness of the 2D nanosheets is around 5 nm, which is consistent with the expected height for a bilayer of **1** (Fig. S2, ESI†). More importantly, a further increase in the volume fraction of the hydrophilic coil of compounds **2** and **3** forced the 2D nanosheets to transform into long (Fig. 2c) and short (Fig. 2d) 1-D nanofibers with a diameter of 5–6 nm. Increasing the volume fraction of hydrophilic polyether units allows oligoether chains to be less confined without sacrificing the anisotropic packing of the aromatic rod segments.[17] Thus, the interface between the hydrophilic and hydrophobic domains changes from a flat interface to a more highly curved interface like that of cylindrical micelles by relieving steric crowding at the interfaces between the aromatic rod and hydrophilic coils.

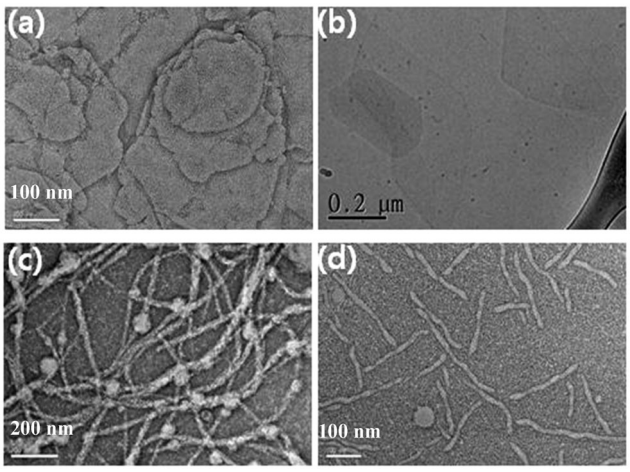

Fig. 2 (a) TEM image from **1**, (b) cryo-TEM image from **1**, (c) TEM image from **2**, (d) cryo-TEM image from **3**, on carbon grid.

In order to investigate the capability of self-assembled nanostructures to functionalize graphite and SWNT into stable dispersion state in aqueous solution, 0.05 wt% (w/v) aqueous solutions of amphiphiles were added to 3 mg of graphite and SWNT followed by sonication for 12 h at room temperature. The resulting dispersions were centrifuged at 12 000 rpm for 30 min and the collected supernatants, having the functionalized graphene and SWNT, were characterized by absorption/emission spectroscopy, Raman spectroscopy and TEM. As shown in Fig. S3 (ESI†), sonication of graphite powder in an aqueous solution of amphiphile **1** afforded a stable dark black dispersion without any sedimentation even after centrifugation, but the black SWNT powder was not dispersed in the same solution. However, an aqueous solution of **3** could form black dispersion with SWNT powder whereas the black graphite powder was not dispersed under the same conditions. This result indicates that the structural dimension of a self-assembled nanostructure plays a key role in the selective functionalization of carbon allotropes.

In order to understand the π–π stacking interaction of the self-assembled nanostructures with carbon allotropes in aqueous solution, we carried out UV absorption and fluorescence spectroscopy. As shown in Fig. S4 (ESI†), the main absorption peaks of **1** and **3** in aqueous solution appeared at 400 nm, respectively. The slight red shift (~4 nm) in the absorption maxima of **1** + G and **3** + SWNT compared to those of **1** and **3** suggested the presence of π–π interactions between the aromatic domain of the nanostructures and the carbon allotrope surfaces. When the dispersed solutions of G and SWNT were excited at 400 nm in aqueous solutions of **1** and **3**, respectively, the fluorescence emission was significantly quenched, indicating that effective electron transfer occurred at the interface between the self-assembled nanostructures and the carbon allotropes.[18]

TEM images obtained from aqueous solutions of **1** + G and **3** + SWNT revealed the presence of 2-D sheet-like structures of G with a dimension of a few hundred nanometers, and long bundles of SWNTs with a few branched individual tubes, respectively (Fig. S5, ESI†). This suggests that the self-assembled nanostructures from **1** and **3** nicely fit the nanosheet and nanofiber

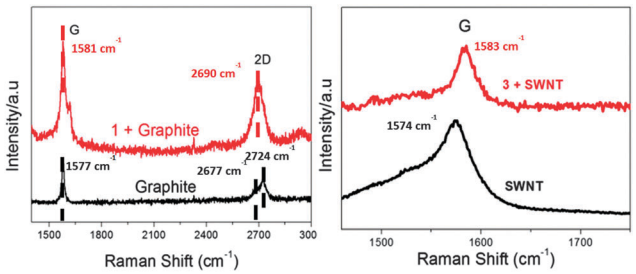

Fig. 3 Raman spectra of **1** + G and **3** + SWNT on quartz plate after drop-casting.

structures of G and SWNT, respectively, to directly functionalize carbon allotropes. Raman scattering is sensitive to the electronic structure of G and SWNT.[17,19]

In order to ascertain the direct exfoliation of the carbon allotropes by the self-assembled nanostructures of the amphiphiles, Raman measurements were carried out on a quartz substrate. As shown in Fig. 3a, a 4 cm^{-1} increase in the Raman shift of the G band was observed for **1** + G (1581 cm^{-1}) compared with that of graphite alone (1577 cm^{-1}) due to the presence of π–π stacking interactions.[20] In addition, the 2D band of **1** + G showed a single and symmetrical Lorentzian peak at 2690 cm^{-1} in contrast to that of graphite. The 2D band of graphite was split into two different sub-peaks, with one small peak at 2677 cm^{-1} and the other large peak at 2724 cm^{-1}. The intensity ratio of **1** + G (I_{2D}/I_G = 0.50) is higher than that of graphite (I_{2D}/I_G = 0.41). All these data indicate that the self-assembled structures of **1** were able to exfoliate graphite to a few layers of graphene.[21] In the case of **3** + SWNT, the Raman G band blue-shifted from 1574 cm^{-1} to 1583 cm^{-1} demonstrating the dissociation of SWNTs from their bundles by the self-assembled structures of **3** (Fig. 3b). Moreover, the section analysis of the AFM images of **1** + G showed that the thickness of the 2-D nanosheets was around 10 nm (Fig. S6, ESI†) and the selected area electron diffraction (SAED) pattern indicated the typical hexagonally arranged lattice of graphene (Fig. S7, ESI†), suggesting that the self-assembled nanostructures from **1** were instantaneously disassembled into the monolayer upon sonication, whereupon its hydrophobic domain of the monolayer were attached to both sides of the 2–4 layers of the graphene sheet (Fig. 1b). No self-assembled structures were formed at high concentrations of **1** (1.5 mg ml^{-1}, 0.15%, w/v) (Fig. S8, ESI†) owing to which G could only be slightly dispersed by **1** (as a small-molecule surfactant); the concentration of dispersed G in concentrated aqueous solution of **1** (1.5 mg ml^{-1}) was lower (0.3 mg/ml) than that (>1 mg ml^{-1}) in the aqueous solution of the self-assembled nanostructures of **1** (0.05%, w/v) (Fig. S3(c), ESI†). Thus, these observations reveal that the 2-D nanosheets self-assembled from **1** exfoliate G more efficiently than the non-self-assembled small-molecule amphiphiles.

Recently, many researchers have utilized G and graphene oxide (GO) as an HTL and an electrode for photovoltaic devices due to their extremely high carrier mobility.[1e,22] However, high costs are needed for depositing a uniform G layer on the substrates, and harsh oxidative chemical exfoliation conditions are also required for obtaining GO flakes from graphite. In this regard, the direct exfoliation of carbon allotropes by self-assembled nanostructures would be a great alternative to the existing methods. We fabricated photovoltaic devices by using a mixture of **1** (self-assembled nanosheet) + G or **3** (self-assembled nanofiber) + CNT and PEDOT:PSS as an HTL at various blending ratios and P3HT : PCBM (1 : 0.8, w/w) as the active layer. Details of the fabrication of photovoltaic devices are described in the ESI.† The photovoltaic, electrical, and morphological data are summarized in Table 1; Table S1 and Fig. S10 (ESI†) displays the *I–V* curves of all devices. The photovoltaic devices based on **3** + CNT in the HTL exhibited similar efficiencies compared to those of the reference device. On the other hand, all devices fabricated using the **1** + G nanostructure in the HTL showed higher efficiencies and similar V_{oc} values compared to those of the reference device at one sun intensity (100 mW cm^{-2}) under simulated AM 1.5G illumination. The short-circuit current (J_{sc}) value of the photovoltaic devices with 10% **1** + G (12.91 mA cm^{-2}) embedded in the HTL was 15% higher than that for the reference device without **1** + G in the HTL (10.49 mA cm^{-2}). Moreover, four-point-probe measurements (Table 1) and the current–voltage measurements of a HTL sandwiched between Al and ITO electrodes (Fig. S11, ESI†) showed that the addition of **1** + G to the PEDOT:PSS HTL resulted in reduced lateral as well as vertical resistance. Thus, these results indicated that the **1** + G self-assembled nanostructure in the HTL contributed to the improvement in the photocurrent of OPVs. However, the fill factor (FF) values were slightly reduced upon increasing the concentration of **1** + G in the PEDOT:PSS layer. To explain this result, we recorded the AFM images of blended films consisting of different ratios of **1** + G and PEDOT:PSS, as shown in Fig. S12 (ESI†). As the concentration of **1** + G increases from 0 to 20 wt%, the roughness (R_{rms}) value also increases from 1.05 to 3.16 nm, respectively. The rough morphology of the HTL at a high concentration of **1** + G could be one of the reasons for the

Table 1 Photovoltaic, electrical, and morphological data

Device	J_{sc} (mA cm^{-2})	V_{oc} (V)	FF	η^a (%)	$R_{sh}{}^b$ (kΩ sq^{-1})	Transmittance^c (%)	R_{rms} (nm)
0% **1** + G	10.49 ± 0.47	0.60 ± 0.01	0.58 ± 0.01	3.63 ± 0.17	635	94.4	1.05
3% **1** + G	11.06 ± 0.38	0.59 ± 0.01	0.57 ± 0.01	3.74 ± 0.12	509	94.5	1.31
5% **1** + G	11.68 ± 0.41	0.60 ± 0.01	0.55 ± 0.01	3.84 ± 0.16	251	94.9	1.63
10% **1** + G	12.91 ± 0.61	0.59 ± 0.01	0.54 ± 0.01	4.17 ± 0.22	178	95.1	2.33
20% **1** + G	12.69 ± 0.34	0.58 ± 0.01	0.50 ± 0.02	3.63 ± 0.12	170	96.3	3.16

[a] Photovoltaic performance parameters are the average values of at least 7 device measurements. [b] Sheet resistance by four-probe measurements. [c] Transmittance at 550 nm.

decrease in FF values in OPVs. Ultraviolet photoelectron spectroscopy (UPS) revealed that the work functions of HTL w/ and w/o self-assembled nanocomposites (**1** + G, **3** + CNT) were similar (Fig. S13, ESI†). Thus, we expect that the addition of the self-assembled structures with carbon allotropes into the PEDOT:PSS layer negligibly affected the interfacial energetics.

In conclusion, we have demonstrated that the 2-D nanosheet and 1-D nanofiber structures can be realized by systematically varying the volume fraction of the hydrophilic coil unit in amphiphilic molecules consisting of a hydrophilic coil and a phenyl-thiophenyl rod segment. We have shown that a high concentration of carbon allotropes can be dispersed in aqueous solution through non-covalent interactions with structurally similar self-assembled nanostructures from amphiphilic molecules; the 2-D nanosheet structure self-assembled from **1** functionalized only 2-D G, whereas the nanofiber structure from **3** exclusively dispersed 1-D SWNT. Furthermore, a mixture of 10% **1** + G and PEDOT:PSS was successfully introduced into the HTL to improve the performance of OPVs by about 15% by increasing the photocurrent. These results demonstrate that the selective non-covalent functionalization of carbon allotropes by self-assembled nanostructures would be an attractive method for the fabrication of optoelectronic devices.

This work was supported by the NRF grant (No. 2013R1A1A2074468) funded by the MSIP and by the New & Renewable Energy Technology Development Program of the KETEP grant (No. 20113020010070) funded by the MKE.

Notes and references

1 (*a*) A. Hirsch, *Nat. Mater.*, 2010, **9**, 868; (*b*) C. N. R. Rao, K. Biswas, K. S. Subrahmanyam and A. Govindaraj, *J. Mater. Chem.*, 2009, **19**, 2457; (*c*) A. K. Geim and K. S. Novoselov, *Nat. Mater.*, 2007, **6**, 183; (*d*) J. K. Wassei, V. C. Tung, S. J. Jonas, K. Cha, B. S. Dunn, Y. Yang and R. B. Kaner, *Adv. Mater.*, 2010, **22**, 897; (*e*) L. Dai, D. W. Chang, J.-B. Baek and W. Lu, *Small*, 2012, **8**, 1130.

2 J. N. Coleman, *Adv. Funct. Mater.*, 2009, **19**, 3680.

3 (*a*) Y.-L. Zhao and J. F. Stoddart, *Acc. Chem. Res.*, 2009, **42**, 1161; (*b*) Y. Liang, D. Wu, X. Feng and K. Müllen, *Adv. Mater.*, 2009, **21**, 1679; (*c*) R. Hao, W. Qian, L. Zhang and Y. Hou, *Chem. Commun.*, 2008, 6576; (*d*) D. Tasis, N. Tagmatarchis, A. Bianco and M. Prato, *Chem. Rev.*, 2006, **106**, 1105.

4 (*a*) P. Kumar, *RSC Adv.*, 2013, **3**, 11987; (*b*) H. S. S. R. Matte, U. Maitra, P. Kumar, B. Govinda Rao, K. Pramoda and C. N. R. Rao, *Z. Anorg. Allg. Chem.*, 2012, **638**, 2617; (*c*) U. Maitra, H. S. S. R. Matte, P. Kumar and C. N. R. Rao, *Chimia*, 2012, **66**, 941; (*d*) P. Kumar, L. S. Panchakarla and C. N. R. Rao, *Nanoscale*, 2011, **3**, 2127.

5 (*a*) L. Vaisman, H. D. Wagner and G. Marom, *Adv. Colloid Interface Sci.*, 2006, **128–130**, 37; (*b*) U. Khan, A. O'Neill, M. Lotya, S. De and J. N. Coleman, *Small*, 2010, **6**, 864; (*c*) Y. Hernandez, M. Lotya, D. Rickard, S. D. Bergin and J. N. Coleman, *Langmuir*, 2009, **26**, 3208; (*d*) J. M. Englert, J. Röhrl, C. D. Schmidt, R. Graupner, M. Hundhausen, F. Hauke and A. Hirsch, *Adv. Mater.*, 2009, **21**, 4265; (*e*) A. Ghosh, K. V. Rao, S. J. George and C. N. R. Rao, *Chem. – Eur. J.*, 2010, **16**, 2700; (*f*) N. Nakashima and T. Fujigaya, *Chem. Lett.*, 2007, **36**, 692; (*g*) X. An, T. Simmons, R. Shah, C. Wolfe, K. M. Lewis, M. Washington, S. K. Nayak, S. Talapatra and S. Kar, *Nano Lett.*, 2010, **10**, 4295.

6 C. Backes, U. Mundloch, A. Ebel, F. Hauke and A. Hirsch, *Chem. – Eur. J.*, 2010, **16**, 3314.

7 (*a*) J. Chen and C. P. Collier, *J. Phys. Chem. B*, 2005, **109**, 7605; (*b*) D. M. Guldi, G. M. A. Rahman, N. Jux, N. Tagmatarchis and M. Prato, *Angew. Chem., Int. Ed.*, 2004, **43**, 5526.

8 (*a*) A. Ciesielski and P. Samori, *Chem. Soc. Rev.*, 2013, **43**, 381; (*b*) M. Lotya, Y. Hernandez, P. J. King, R. J. Smith, V. Nicolosi, L. S. Karlsson, F. M. Blighe, S. De, Z. Wang, I. T. McGovern, G. S. Duesberg and J. N. Coleman, *J. Am. Chem. Soc.*, 2009, **131**, 3611.

9 D.-W. Lee, T. Kim and M. Lee, *Chem. Commun.*, 2011, **47**, 8259.

10 C. Ehli, C. Oelsner, D. M. Guldi, A. Mateo-Alonso, M. Prato, C. Schmidt, C. Backes, F. Hauke and A. Hirsch, *Nat. Chem.*, 2009, **1**, 243.

11 H. Murakami, T. Nomura and N. Nakashima, *Chem. Phys. Lett.*, 2003, **378**, 481.

12 S. Sampath, A. N. Basuray, K. J. Hartlieb, T. Aytun, S. I. Stupp and J. F. Stoddart, *Adv. Mater.*, 2013, **25**, 2740.

13 Y.-b. Lim, K.-S. Moon and M. Lee, *J. Mater. Chem.*, 2008, **18**, 2909.

14 (*a*) H.-J. Kim, T. Kim and M. Lee, *Acc. Chem. Res.*, 2010, **44**, 72; (*b*) X. Zhang and C. Wang, *Chem. Soc. Rev.*, 2011, **40**, 94; (*c*) S. Förster and T. Plantenberg, *Angew. Chem., Int. Ed.*, 2002, **41**, 688.

15 (*a*) A. Hlel, A. Mabrouk, M. Chemek and K. Alimi, *Spectrochim. Acta, Part A*, 2012, **99**, 126; (*b*) P. Hermet, S. Lois-Sierra, J. L. Bantignies, S. Rols, J. L. Sauvajol, F. Serein-Spirau, J. P. Lère-Porte and J. J. E. Moreau, *J. Phys. Chem. B*, 2009, **113**, 4197.

16 J.-K. Kim, E. Lee, Z. Huang and M. Lee, *J. Am. Chem. Soc.*, 2006, **128**, 14022.

17 J.-H. Ryu, D.-J. Hong and M. Lee, *Chem. Commun.*, 2008, 1043.

18 L. Li, C. Tedeschi, D. G. Kurth and H. Möhwald, *Chem. Mater.*, 2004, **16**, 570.

19 (*a*) E. A. Obraztsova, A. V. Osadchy, E. D. Obraztsova, S. Lefrant and I. V. Yaminsky, *Phys. Status Solidi*, 2008, **245**, 2055; (*b*) A. Ghosh, K. V. Rao, R. Voggu and S. J. George, *Chem. Phys. Lett.*, 2010, **488**, 198.

20 N. O. Weiss, H. Zhou, L. Liao, Y. Liu, S. Jiang, Y. Huang and X. Duan, *Adv. Mater.*, 2012, **24**, 5782.

21 D. Graf, F. Molitor, K. Ensslin, C. Stampfer, A. Jungen, C. Hierold and L. Wirtz, *Nano Lett.*, 2007, **7**, 238.

22 (*a*) M. P. Ramuz, M. Vosgueritchian, P. Wei, C. Wang, Y. Gao, Y. Wu, Y. Chen and Z. Bao, *ACS Nano*, 2012, **6**, 10384; (*b*) J. Kim, V. C. Tung and J. Huang, *Adv. Energy Mater.*, 2011, **1**, 1052; (*c*) X. Huang, Z. Zeng, Z. Fan, J. Liu and H. Zhang, *Adv. Mater.*, 2012, **24**, 5979; (*d*) J. Liu, Y. Xue, Y. Gao, D. Yu, M. Durstock and L. Dai, *Adv. Mater.*, 2012, **24**, 2228; (*e*) I. P. Murray, S. J. Lou, L. J. Cote, S. Loser, C. J. Kadleck, T. Xu, J. M. Szarko, B. S. Rolczynski, J. E. Johns, J. Huang, L. Yu, L. X. Chen, T. J. Marks and M. C. Hersam, *J. Phys. Chem. Lett.*, 2011, **2**, 3006; (*f*) V. C. Tung, J. Kim, L. J. Cote and J. Huang, *J. Am. Chem. Soc.*, 2011, **133**, 9262.

